FINITE ELEMENT SIMULATION OF PIPE-IN-PIPE SYSTEMS INSTALLED ON AN UNEVEN SEABED

F. Van den Abeele
Fugro GeoConsulting Belgium
Brussels, Belgium

Q. De Ville
Université Catholique de Louvain
Louvain-la-Neuve, Belgium

T. Giagmouris
Genesis Oil and Gas
Houston, US

E. Onya
Cranfield University
Cranfield, UK

J. Njuguna
Robert Gordon University
Aberdeen, UK

ABSTRACT

Thanks to their exceptional thermal insulation capability, Pipe-in-Pipe (PIP) systems are well suited for the transportation of hydrocarbons at high pressure and high temperatures (HP/HT), preventing hydrate formation and ensuring high discharge temperatures at the arrival facility. This is the reason why PIP systems are increasingly being used in the design of HP/HT flowlines.

There are two types of PIP systems used in the offshore industry: (i) *fully bonded* PIP, in which the entire annulus is filled with insulation material like PU, and (ii) *unbonded* PIP, in which the insulation is achieved by wrapping standard size insulation pads onto the inner pipe.

When a Pipe-in-Pipe system is installed on an uneven seabed, the inner pipe can experience significant bending due to internal pressure and temperature of the conveyed fluid. This may trigger contact between the inner and outer pipe.

In this paper, different numerical approaches to simulate the structural response of a pipe-in-pipe system are reviewed and compared. The fully bonded PIP can be simulated using an equivalent diameter approach, replacing both pipes by one single pipe with an equivalent mass and bending stiffness. This approach has been pursued to evaluate the mechanical response of a PIP system in a free span. A formulation is presented to reconstruct the stress distributions in the inner and outer pipes based on the strains and bending moments calculated for the equivalent cross section. The results show that the equivalent pipe section can be used for on-bottom roughness analysis and free span assessment of fully bonded Pipe-in-Pipe systems.

INTRODUCTION TO PIPE-IN-PIPE SYSTEMS

Pipe-in-Pipe systems consist of an inner pipe, conveying the hydrocarbons and hence exposed to the internal pressure and temperature, and an outer (carrier) pipe, withstanding the external pressure. The annulus between inner and outer pipe is filled with dry insulation material like mineral wool, polyurethane foam, aerogel, granular or microporous materials or ceramics. With such design, Pipe-in-Pipe systems can achieve excellent insulation capabilities, allowing for an Overall Heat Transfer Coefficient (OHTC) or U-value lower than 1.0 W/m^2K.

Figure 1: Cross section of a Pipe-in-Pipe system [1]

Thanks to their exceptional thermal insulation capability, Pipe-in-Pipe systems are well suited for the transportation of hydrocarbons at high pressure and high temperatures (HP/HT), preventing hydrate formation and ensuring high discharge temperatures at the arrival facility. This is the reason why PIP systems are increasingly being used in the design of HP/HT flowlines.

Today, Pipe-in-Pipe is widely used in the North Sea, Africa, the Pacific and the Gulf of Mexico. As there is a market pull for deepwater HP/HT pipelines, and field developments requiring long tie-backs, the importance of Pipe-in-Pipe systems is expected to grow significantly in the coming years.

In addition, Pipe-in-Pipe systems can provide a solution for cryogenic transfer lines to transport Liquified Petroleum Gas (LPG) or Liquified Natural Gas (LNG). Subsea LNG pipelines can provide a cost-effective alternative for ship carriers, provided cryogenic materials (i.e. high nickel alloys) are used for pipe material, forgings and welding consumables [2]. For such applications, a triple wall system can be envisaged to ensure high-efficiency thermal insulation.

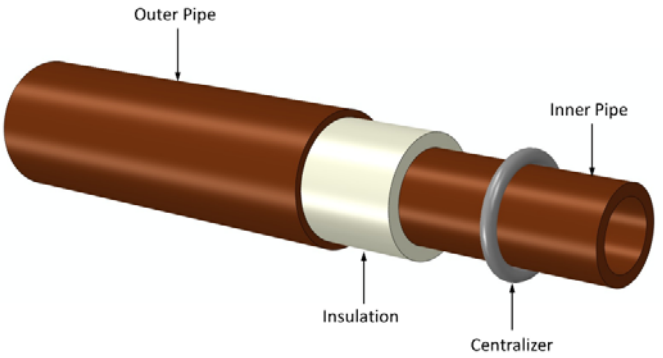

Figure 2: Typical Pipe-in-Pipe Configuration

There are two types of PIP systems used in the offshore industry: (i) *fully bonded* or compliant PIP, in which the entire annulus is filled with insulation material like PU, and (ii) *unbonded* or *non-compliant* PIP, in which the insulation is achieved by wrapping standard size insulation pads onto the inner pipe. In compliant PIP systems, load transfer is continuous and the inner and outer pipe deform uniformly. In non-compliant PIP systems, the inner and outer pipes can move relative to each other.

A typical Pipe-in-Pipe configuration is shown in Figure 2. A PIP comprises bulkheads, water stops and centralizers. The end *bulkhead* is designed to connect the inner pipe to the outer pipe at each pipeline termination. Intermediate bulkheads may be required for reeled PIP to allow the top tension to be transferred between the outer pipe and the inner pipe.

The fundamental driver for *water stops* is to avoid flooding of the entire annulus of a PIP due to a single defect in the outer pipe. Hence, water stops are installed to limit the pipeline length exposed to flooding by failure of puncture of the outer pipe. Spacing of the water stops is a compromise between repair costs, temperature loss from the flooded segment and availability of spare materials.

Spacers or *centralizers* are polymeric rings clamped on the inner pipe at regular intervals to transfer loads between the inner and outer pipe and to prevent possible damage (like abrasion or crushing) of the insulation material. As the centralizers act as a heat sink, with thermal conductivity an order of magnitude higher than the insulation material, they reduce the overall thermal performance of PIP systems. Hence, the spacing has to be maximized (typically two meters for reeled pipes and up to six meters for S-lay and J-lay installation).

A comprehensive overview of thermal management and material issues related to Pipe-in-Pipe flowline systems is given in [3]. Design considerations and challenges are listed in [4], and the reader is referred to [5] for an overview on qualification testing of deepwater PIP for extra high pressure high temperature (XHPHT) conditions.

REVIEW OF NUMERICAL MODELS FOR PIPE IN PIPE

Jukes, Sun et. al. have published a substantial body of work [3-9] on Pipe-in-Pipe systems, driven by the research and development program of JP Kenny to introduced PIP for deepwater HP/HT flowlines in the Gulf of Mexico.

In their landmark OMAE paper [7], they introduce an Abaqus finite element model to simulate unbonded (sliding) Pipe-in-Pipe systems. The inner and outer pipe are modelled separately using hybrid pipe elements (PIPE31H), which are the most appropriate beam elements to model long, slender pipelines. Initially, the heart lines of both pipes share the same position. An elastic connector element (CONN3D2) was used to simulate bonding of the end bulkhead and the intermediate load sharing bulkheads at specified locations. The interaction between the centralizers, which are clamped on the inner pipe at a designated spacing, and the outer pipe was modelled using tube-to-tube contact elements (ITT), which allow relative axial and lateral movements constrained by clearance and friction. Hence, the ITT contact elements can accurately simulate the contact reaction forces and corresponding load transfer (through the centralizer) between the inner and the outer pipe. This ‘global’ finite element model is subsequently used to simulate the load response of unbonded PIP systems from the J-lay installation to HP/HT operation.

In an accompanying paper [8], the same authors address the propagating limit state of Pipe-in-Pipe flowlines, based on the pioneering work of Kyriakides [10-12]. For that analysis, both inner and outer pipe were modelled using shell elements.

In their 2008 OTC paper [9], the authors compare the 'global' finite element model using beam elements and ITT contact elements with the results of a 'local' finite element model, where (S4R) shell elements are used to model the inner and outer pipe, and 3D (C3D8R) solid element are used to represent the spacers and bulkheads. Both the global and local finite element models are applied to investigate the limit state design of XHPHT Pipe-in-Pipe flowlines. The limit state design covered local buckling, hoop stress ratcheting, strain capacity and low cycle fatigue. The local and global finite element models produced comparable results [7] in terms of pipeline stress response.

Different limit states for Pipe-in-Pipe are investigated by other authors [13-20] as well. In [13], the authors explore the potential failure envelope of the inner pipe for axial compression loading. The inner and outer pipes were modelled individually using beam elements to capture the global response. A static finite element analysis was performed to sequentially apply –using a pseudo-time scale- various installation, weight, pressure and temperature loadings. The authors highlight that the beam elements, commonly used in global flowline (and PIP) analysis will fail to capture the strain localization characteristics in regions of the (inner) pipe experiencing gross yielding and subsequent collapse.

The phenomenon of Pipe-in-Pipe walking is addressed in [14], using an Abaqus finite element model where the inner and outer pipes are modelled using hybrid beam elements and tube-to-tube contact elements. The flat seabed is modelled as a rigid plan. The non-linear spacer-pipe friction and pipe-soil friction was identified as the mechanism of PIP walking under thermal transients. To mitigate the walking behaviour, the authors suggest to reduce the spacer-pipe friction, to gradually heat up the pipe, and/or to depressurize the line during shutdown.

The structural response and design criteria for global buckling of a Pipe-in-Pipe system are described in [15]. A Pipe-in-Pipe system will experience global buckling when the compressive effective axial force exceeds the buckling capacity. A simplified 2D FE model is presented, where pressure and temperature are sequentially introduced in the inner pipe. The inner pipe builds up compressive forces until global buckling occurs: the whole PIP system moves out of position and initiates a global buckle. Beyond the onset of global buckling, the outer pipe develops tension, counteracting the development of a buckle, whereas the inner pipe continues to increase compressive forces, keeping the total effective axial force of the PIP system at a fairly constant level in post buckling condition. For buried PIP systems, especially where the inner pipe is under HT/HP conditions, one of the governing design aspects may be combined loading due to axial compression and internal pressure. The authors recognize [15] that no explicit design criterion exists in the offshore pipeline design codes, and propose to solve the design challenges using a stochastic design approach outlined in [16].

An extensive yet comprehensive mathematical model to calculate thermal expansion of Pipe-in-Pipe systems is presented in [17]. The paper is concerned with non-compliant systems and investigates a structurally symmetric Pipe-in-Pipe with equidistant regular spacers along its length (to avoid intermediate contact between inner and outer pipe) and a bulkhead at each end. A complete mathematical model is provided for the bulkhead forces and axial displacement, inner pipe axial force and outer pipe tension under temperature variations of both the inner and the outer pipe. The analytical results are in good agreement with the finite element analyses reported in [18].

In [19], a Pipe-in-Pipe system without centralizers is modelled to calculate the critical (compressive) effective axial forces needed to trigger sinusoidal and –subsequently- helical bucking of the inner flowline. Again, Abaqus PIPE31 elements are used to model both the inner and outer pipes, and tube-to-tube contact elements (ITT) are applied to simulate friction. This finite element model could simulate the complex deformation pattern associated with helical buckling of the inner pipe, and was shown to predict values for critical buckling loads in good agreement with published data.

A local, fully 3D finite element model of a Pipe-in-Pipe system using brick elements and complete representation of the elasto-plastic material properties of all metallic components was presented in [20]. Although this approach is computationally expensive and hence not suited to analyze the global response of PIP systems, it can provide a powerful tool to study local effects like strain concentrations and the development of localized plastic strains during Steep S-lay installation of PIP systems in deep water.

RESPONSE OF PIPE IN PIPE SYSTEM IN FREE SPAN

In this paper, we intend to study the response of Pipe-in-Pipe systems when installed on an uneven seabed in order to identify free spans which may be susceptible to vortex induced vibrations and hence fatigue damage. Numerical simulations of the mechanical response of a Pipe-in-Pipe in a span were recently published by Giagmouris et. al. [21-22].

In this analysis, they present the results of an academic example on an artificial, stepped seabed with the dimensions shown in Figure 3: the total seabed length is 1256 m, with a gap of 36 m to introduce a symmetric free span.

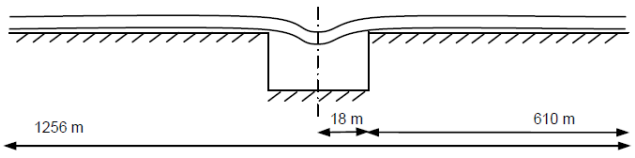

Figure 3: Pipeline spanning on an artificial seabed

The PIP system under consideration consists of an X65 inner pipe with outer diameter OD_{in} = 219 mm (8.625") and wall thickness t_{in} = 29 mm, and an X65 outer carrier pipe with diameter OD_{out} = 324 mm (12.75") and wall thickness t_{out} = 18 mm. This configuration leads to an annulus of 34.4 mm (1.35") and, assuming no insulation and empty installation, an initial submerged weigth of 1.84 kN/m.

Table 1: Geometric properties of Pipe-in-Pipe system [21]

Pipe	Diameter [mm]	Wall thickness [mm]	D/t [-]
Inner	219	29	7.55
Outer	324	18	18

The geometric properties of this Pipe-in-Pipe system are summarized in Table 1. The X65 steel grade has a Young's modulus of E = 210 GPa, a contraction coefficient of ν= 0.3, a yield stress of σ_y = 450 MPa, a density of ρ = 7850 kg/m³ and a thermal expansion coefficient of α = 12.10^{-6} m/mK.

Four different types of finite element models [22] were compared:

1. Both pipes modelled as (PIPE31H) pipe elements, where Multi Point Constraints (MPC) keep the inner pipe on the axis of the outer pipe. Using such constraints, both pipe remain concentric but can allow for relative axial displacement.
2. Similar as (1) but using elbow elements for the sagging PIP section, where the bending moments are more pronounced.
3. Both pipes modelled as (PIPE31H) pipe elements without constraints on their degrees of freedom. Frictional contact and load transfer between the inner and the outer pipe is governed by tube-to-tube contact (ITT) elements.
4. Both pipes modelled using (S4R) shell elements, assuming frictional contact between mating surfaces.

The most important conclusions from the analyses presented in [21-22] read:

- Elbow elements should only be used when ovalization is significant, i.e. locations where substantial bending can be expected.
- Shell elements are computationally expensive and provide little added value when studying the mechanical response of a Pipe-in-Pipe system in a free span
- Similar to shell elements, tube-to-tube contact elements allow for interaction between the inner and the outer pipe, but at the expense of a higher computational effort
- The PIP model with the concentric constraint leads to an elegant and simple model which is reasonably accurate and cost effective for modelling PIP during conceptual design.

The latter conclusion favours the use of simple beam element models to simulate Pipe-in-Pipe and paves the way for a 1D approach to model compliant PIP systems in free spans.

EQUIVALENT CROSS SECTION FOR COMPLIANT PIP

This paper wants to explore finite element simulation of Pipe-in-Pipe systems installed on an uneven seabed using the SAGE Profile software suite for offshore pipeline analysis. SAGE Profile is the industry standard software for on bottom roughness. A comprehensive overview of the software is given in [23], and its application to fatigue analysis for free spanning pipelines subjected to vortex induced vibrations was presented in [24]. SAGE Profile has been tailored to assist the pipeline engineer during offshore pipeline design. Using a transient dynamic explicit solver, it can accurately mimic the actual pipeline installation process, like shown in Figure 4.

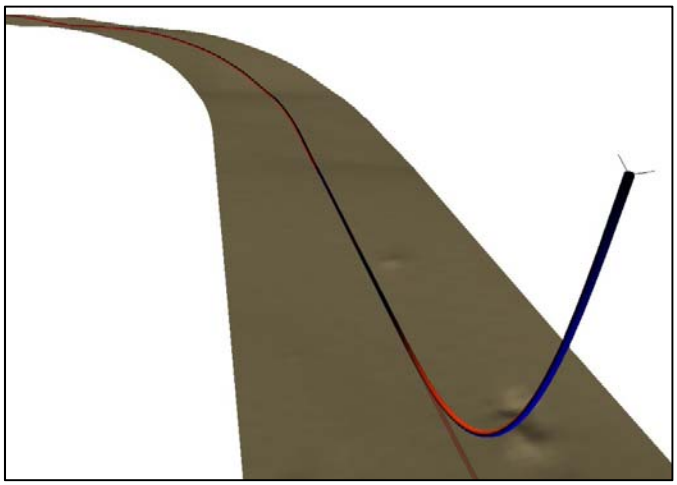

Figure 4: SAGE Profile offshore pipeline simulation

However, the finite element solver has been designed for circular, single walled trunklines and flowlines. As a result, the default elements are Bernoulli beams where the cross section is described by one steel layer (defined by its outer diameter and wall thickness), which can be complemented by a layer of (corrosion or concrete) coatings.

In order to simulate a (compliant, fully bonded) Pipe-in-Pipe system, an equivalent single wall cross section has to be defined with similar bending stiffness, axial stiffness and mass as the global PIP system. Such an equivalent cross section can capture the global mechanical response of the original Pipe-in-Pipe system, provided the following assumptions are satisfied:

- Both inner and outer pipes have the same curvature during different load stages, which can be justified by the centralizer spacing
- There is no relative axial movement between both pipes
- The external hydrostatic pressure is fully born by the outer pipe, and the inner pipe is not affected
- The inner pipe withstands internal pressure of the conveyed hydrocarbons, without affecting the outer pipe
- The analysis is linear elastic, which is acceptable for general free span calculations

As the assumptions hold for free span assessment of a fully bonded (compliant) Pipe-in-Pipe system, we can use SAGE Profile for this purpose, using judiciously chosen values for outer diameter OD_{eq} and wall thickness t_{eq} of the equivalent cross section. Indeed, the equivalent cross section should have the same bending stiffness as the original PIP system, which can be achieved by imposing a requirement on the (area) moment of inertia

$$I_{eq} = I_{in} + I_{out} = \frac{\pi}{64}\left(OD_{eq}^4 - ID_{eq}^4\right) \tag{1}$$

where I_{in} and I_{out} represent the moment of inertia for the inner and outer pipe respectively. Similarity of both mass and axial stiffness is achieved by superposition of the cross sectional area

$$A_{eq} = A_{in} + A_{out} = \frac{\pi}{4}\left(OD_{eq}^2 - ID_{eq}^2\right) \tag{2}$$

with A_{in} and A_{out} the cross sectional area of the inner and outer pipe respectively. The set of equations (1)-(2) allows deriving the inner and diameter ID_{eq} and OD_{eq} for the equivalent cross section. Indeed, using the notations

$$A = \frac{4}{\pi}\left(A_{in} + A_{out}\right) \quad \text{and} \quad I = \frac{64}{\pi}\left(I_{in} + I_{out}\right) \tag{3}$$

it can easily be shown that

$$OD_{eq} = \sqrt{\frac{I + A^2}{2A}} \quad \text{and} \quad ID_{eq} = \sqrt{\frac{I - A^2}{2A}} \tag{4}$$

Realizing that $OD_{eq} = ID_{eq} + 2\,t_{eq}$, the Pipe-in-Pipe system defined in [21-22] and summarized in Table 1, can be represented by an equivalent cross section with outer diameter OD_{eq}= 295.7 mm and wall thickness t_{eq}= 43.7 mm. In the SAGE Profile pipeline input, a mass-less coating with thickness

$$t_c = \frac{OD_{out} - OD_{eq}}{2} = 14 \text{ mm} \tag{5}$$

is added to obtain the same buoyancy as the initial PIP an hence to correctly reproduce the submerged weight of the equivalent cross section.

The fully restrained effective axial force of a Pipe-in-Pipe section can be written as

$$F_{eff} = F_{tw} + F_{int} - F_{ext} \tag{6}$$

where

$$F_{int} = -p_{int}\,A_{int} \tag{7}$$

is the axial force induced by the internal pressure p_{int} on the surface $A_{int} = \frac{\pi}{4}\,ID_{in}^2$

$$F_{ext} = -p_{ext}\,A_{ext} \tag{8}$$

is the axial force induced by the external (hydrostatic) pressure p_{ext} on the surface $A_{ext} = \frac{\pi}{4}\,OD_{out}^2$, and the true wall force

$$F_{tw} = F_{in} + F_{out} \tag{9}$$

comprises the contribution of the inner pipe

$$F_{in} = -EA_{in}\,\alpha\,\Delta T_{in} + \nu\,\frac{p_{int}\,ID_{in}}{2\,t_{in}}\,A_{in} \tag{10}$$

and the outer pipe

$$F_{in} = -EA_{out}\,\alpha\,\Delta T_{out} + \nu\,\frac{p_{ext}\,OD_{out}}{2\,t_{out}}\,A_{out} \tag{11}$$

where ΔT_{in} and ΔT_{out} are the temperature gradients experienced by the inner and outer pipe respectively. Combining (6)-(11), the effective axial force for a fully restrained Pipe-in-Pipe system can be re-written as

$$\begin{aligned} F_{eff} = & -E\alpha\left(A_{in}\Delta T_{in} + A_{out}\Delta T_{out}\right) \\ & + \frac{\nu}{2}\left(\frac{p_{int}\,ID_{in}\,A_{in}}{t_{in}} + \frac{p_{out}\,OD_{out}\,A_{out}}{t_{out}}\right) \\ & - \frac{\pi}{4}\left(p_{int}\,ID_{in}^2 - p_{ext}\,OD_{out}^2\right) \end{aligned} \tag{11}$$

To ensure compatibility of the temperature and pressure induced loads in the original Pipe-in-Pipe system and the equivalent cross section, the effective axial force in the equivalent PIP must be the same as (11). This condition is fulfilled, provided that

$$F_{eff} = -EA_{eq}\alpha\Delta T_{eq} - \nu\,A_{eq}\,\frac{p_{int}^{eq}\,ID_{eq} - p_{ext}^{eq}\,OD_{eq}}{OD_{eq} - ID_{eq}} \tag{12}$$

If we set the internal and external pressure in the equivalent PIP section to zero, i.e. $p_{int}^{eq} = 0 = p_{out}^{eq}$, the equivalent temperature gradient

$$\Delta T_{eq} = -\frac{F_{eff}}{EA_{eq}\alpha} \tag{13}$$

produces the same effective axial force as (11) when applied to the equivalent PIP cross section.

Finite element simulations for the equivalent PIP section were performed with SAGE Profile, using the stepped seabed proposed in [21-22] and shown in Figure 3 as a benchmark. The soil properties are chosen to reflect the conditions suggested in [22], i.e. lateral factor of $\mu_{lat} = 0.3$ and an axial friction factor of $\mu_{ax} = 0.46$. The lateral friction factor does not influence the free span assessment, but the axial friction between the seabed and the PIP governs the amount of feed-in.

For the vertical soil spring, [22] only suggests an "assumed embedment" of 0.5 OD_{eq}. For this analysis at hand, we assume that the vertical soil reaction can be described as a very soft clay with an undrained shear strength of C_u = 10 kPa and a submerged unit weight of $\gamma_s = 7.5$ kN/m³. The vertical soil spring reflects the bearing capacity Q_u and for clays, DNV-RP-F105 [25] recommends

$$Q_u(z_p) = \left(5.14\, C_u + \gamma_s\, z_p\right) B(z_p) \tag{14}$$

where z_p is the pipe penetration, and

$$B(z_p) = \begin{cases} 2\sqrt{z_p(OD_{tot} - z_p)} & 0 \le z_p \le OD_{tot}/2 \\ OD_{tot} & \text{otherwise} \end{cases} \tag{15}$$

the bearing width, with $OD_{tot} = OD_{eq} + 2t_c$ the total outer diameter of the equivalent PIP cross section.

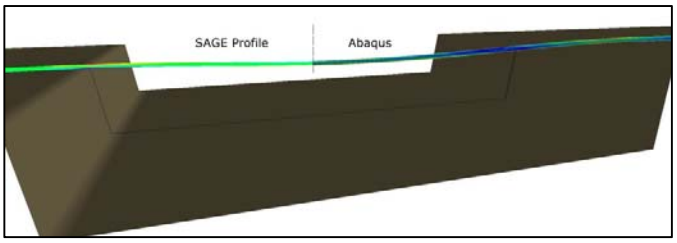

Figure 5: Equivalent Pipe-in-Pipe sagging in a free span

The laydown analysis for the equivalent Pipe-in-Pipe section was performed using both SAGE Profile and Abaqus. For all finite element analyses, an element length of 1 meter was selected. The predicted mechanical response of the PIP system sagging in the free span is superimposed for both solvers in Figure 5.

The predicted vertical displacement of the Pipe-in-Pipe system is shown in Figure 6 for

- The SAGE Profile equivalent PIP laydown simulation
- A similar Abaqus run for the equivalent PIP cross section
- The approach pursued in [21-22], i.e. an Abaqus Pipe-in-Pipe simulation modelling both inner and outer pipes with PIPE31H elements, and applying ITT tube-to-tube contact elements

The results show that the vertical displacements predicted by the Abaqus simulations (Pipe-in-Pipe and equivalent cross section) coincide, which indicates that the equivalent cross section described by (4) indeed can be applied to predict the mechanical response of compliant Pipe-in-Pipe systems. The vertical displacements predicted using SAGE Profile are slightly higher (difference < 5%), which could be attributed to the pipeline laydown algorithm [23].

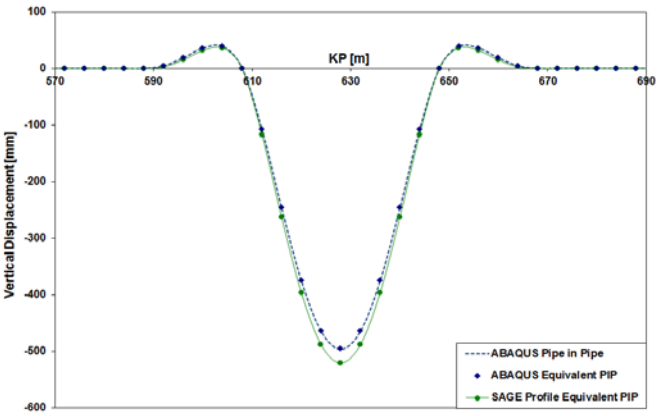

Figure 6: Predicted vertical displacement PIP in free span

DECOMPOSITION OF EQUIVALENT PIP STRESSES

The SAGE Profile laydown simulations using the equivalent cross section (4) and the equivalent temperature gradient (13) yield the pipeline axial strains ε_{eq} and bending moments M_{eq}. These state variables allow reconstructing the stress distributions in the inner and outer pipe of the original Pipe-in-Pipe system.

Indeed, the axial true wall stresses in the inner pipe can be assessed using the fully restrained true wall stresses and the computed axial strains:

$$\sigma_{in}^{ax} = -E\,\alpha\,\Delta T_{in} + \nu\,\frac{p_{int}\,ID_{in}}{2\,t_{in}} + \varepsilon_{eq}E \tag{16}$$

and, similarly, for the outer pipe:

$$\sigma_{out}^{ax} = -E\,\alpha\,\Delta T_{out} + \nu\,\frac{p_{ext}\,OD_{out}}{2\,t_{out}} + \varepsilon_{eq}E \tag{17}$$

The corresponding axial forces can hence be calculated as

$$F_{in}^{ax} = \sigma_{in}^{ax} A_{in} \quad \text{and} \quad F_{out}^{ax} = \sigma_{out}^{ax} A_{out} \tag{18}$$

Since we assume that the inner and outer pipe have the same curvature, the maximum bending stresses can readily obtained as

$$\sigma_{in}^{b} = \frac{OD_{in}\,M_{eq}}{2\,I_{eq}} \quad \text{and} \quad \sigma_{out}^{b} = \frac{OD_{out}\,M_{eq}}{2\,I_{eq}} \tag{19}$$

The bending moments in the inner and outer pipe cross-sections are

$$M_{in} = M_{eq}\,\frac{I_{in}}{I_{eq}} \quad \text{and} \quad M_{out} = M_{eq}\,\frac{I_{out}}{I_{eq}} \tag{20}$$

The wall stresses are then obtained by combining axial and bending stresses:

$$\sigma_{in} = \sigma_{in}^{ax} \pm \sigma_{in}^{b} \quad \text{and} \quad \sigma_{out} = \sigma_{out}^{ax} \pm \sigma_{out}^{b} \tag{21}$$

Assuming that the shear strength τ is proportionally distributed over the inner and outer pipe cross sections, and using thin-walled pipe assumptions, the equivalent stresses in the outer pipe can be written as

$$\sigma_{out}^{eqv} = \sqrt{\sigma_{out}^{2} + (\sigma_{out}^{h})^{2} - \sigma_{out}\sigma_{out}^{h} + 3\tau^{2}} \tag{22}$$

where

$$\sigma_{out}^{h} = -\frac{p_{ext} OD_{out}}{2\, t_{out}} \tag{23}$$

is the hoop stress in the outer pipe. In Figure 7, the equivalent stresses (22) calculated for the outer pipe based on the strains and bending moments of the equivalent cross section are compared with the results from the Pipe-in-Pipe simulations using Abaqus.

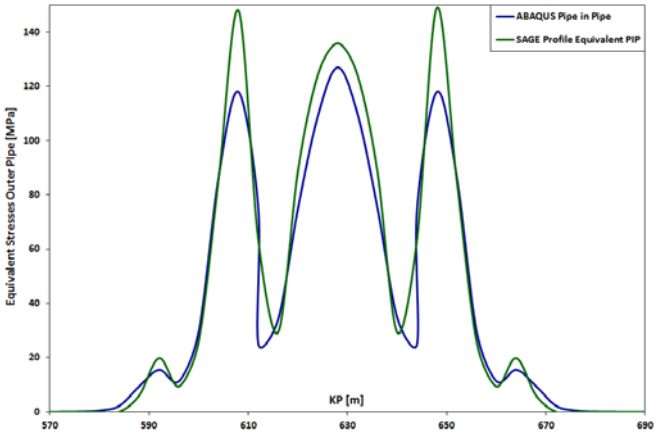

Figure 7: Equivalent stresses in the outer pipe

The results show a good agreement, although SAGE Profile predicts higher contact forces at the span shoulders. This can be attributed to the vertical soil reaction, which is calculated using a non-linear soil spring in SAGE Profile, whereas Abaqus uses a pressure/overclosure to simulate pipeline embedment and soil reaction forces.

Similar to (22), the equivalent stresses in the inner pipe can be written as

$$\sigma_{in}^{eqv} = \sqrt{\sigma_{in}^{2} + (\sigma_{in}^{h})^{2} - \sigma_{in}\sigma_{in}^{h} + 3\tau^{2}} \tag{24}$$

with

$$\sigma_{in}^{h} = \frac{p_{int} ID_{in}}{2\, t_{in}} \tag{25}$$

the hoop stress in the inner pipe.

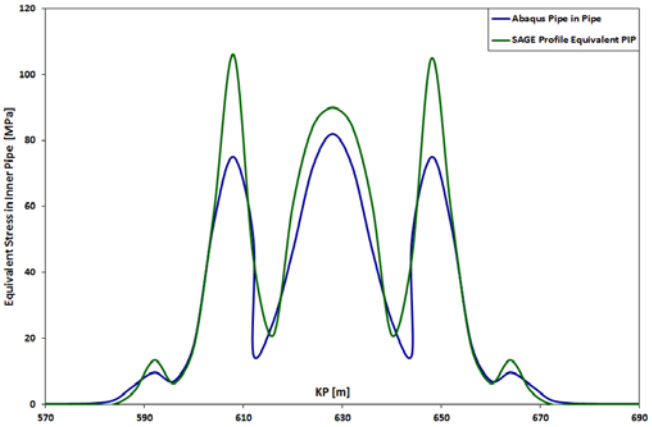

Figure 8: Equivalent stresses in the inner pipe

The equivalent stresses (24) calculated for the inner pipe based on the strains and bending moments of the equivalent cross section are compared with the results from the Pipe-in-Pipe simulations using Abaqus. Again, the results show fairly good agreement except for the regions in close proximity to the span shoulders.

It should be noted that the inner pipe, with a ratio of diameter over wall thickness $D/t = 7.55$, can no longer be modelled as a thin-walled pipe, hence invalidating the assumption (25). For free span assessment, the approach is still justified provided the contribution of the hoop stress does not dominate the mechanical response of the pipe. For thermal expansion analysis and global buckling simulations of high pressure pipelines, however, the thick-walled formulation should be used [25].

The analysis results, presented in this paper, indicate that the proposed equivalent pipe section can be used for on-bottom roughness analysis and free span assessment of fully bonded Pipe-in-Pipe systems.

CONCLUSIONS

In this paper, different numerical approaches to simulate the structural response of a Pipe-in-Pipe system were reviewed and compared. An equivalent diameter approach was proposed to simulate fully bonded (compliant) Pipe-in-Pipe systems, replacing both pipes by one single pipe with equivalent mass and stiffness. This approach was pursued to simulate the mechanical response of a PIP system in a free span. A formulation was presented to reconstruct the stress distributions in the inner and outer pipes based on the strains and bending moments calculated for the equivalent cross section. The results, presented in this paper, show that the equivalent pipe section can be used for on-bottom roughness analysis and free span assessment of fully bonded Pipe-in-Pipe systems.

REFERENCES

[1] Lee J., Introduction to Offshore Pipelines and Risers (2008)

[2] Phalen T., Prescott N., Zhang J. and Findlay T., Update on Subsea LNG Pipeline Technology, Proceedings of the Offshore Technology Conference, OTC-18542 (2007)

[3] Jukes P., Sing B., Garcia J. and Delille F., Critical Thermal, Corrosion and Material Issues Related to Flowline Pipe-in-Pipe (PIP) Systems, Proceedings of the 18th Ocean and Polar Engineering Conference, ISOPE-2008-TPC-297 (2008)

[4] Jukes P., Eltahar A., Sun J. and Harrison G., Extra High Pressure High Temperature (XHPHT) Flowlines – Design Considerations and Challenges, Proceedings of the 28th International Conference on Ocean, Offshore and Arctic Engineering, OMAE2009-79537 (2009)

[5] Jukes P., Delille F. and Harrison G., Deepwater Pipe-in-Pipe (PIP) Qualification Testing for 350°F Service, Proceedings of the 3rd International Offshore Pipeline Forum, IPF2008-922 (2008)

[6] Banneyake R., Sun J., Jukes P. and Chen J., Analytical Estimation of Pretension Requirements to Inner Pipe of Pipe-in-Pipe Flowline in Ultra Deep Water using J-Lay Installation, Proceedings of the Offshore Technology Conference, OTC-20256 (2009)

[7] Sun J. and Jukes P., From Installation to Operation – A Full-scale Finite Element Modelling of Deepwater Pipe-in-Pipe Systems, Proceedings of the 28th International Conference on Ocean, Offshore and Arctic Engineering, OMAE2009-79519 (2009)

[8] Wang H., Sun J. and Jukes P., Finite Element Analysis of a Laminate Internal Buckle Arrestor for Deepwater Pipe-in-Pipe Flowlines, Proceedings of the 28th International Conference on Ocean, Offshore and Arctic Engineering, OMAE2009-79520 (2009)

[9] Jukes P., Sun J. and Eltaher A., Investigation into the Limit State Design of XHPHT PIP Flowlines using Local and Global Finite Element Analysis Methods, Proceedings of the Offshore Technology Conference, OTC-19372 (2008)

[10] Kyriakides S., Buckle Propagation in Pipe-in-Pipe Systems, Part I: Experiments, International Journal of Solids and Structures, vol. 39, pp. 351-366

[11] Kyriakides S. and Vogler T., Buckle Propagation in Pipe-in-Pipe Systems, Part II: Analysis, International Journal of Solids and Structures, vol. 39, pp. 367-392

[12] Kyriakides S. and Netto T.A., On the Dynamic Propagation and Arrest of Buckles in Pipe-in-Pipe Systems, International Journal of Solids and Structures, vol. 41, pp. 5463-5482 (2004)

[13] Harrison G. and McCarron B., Potential Failure Scenario for High Temperature Deep Water Pipe-in-Pipe, Proceedings of the Offshore Technology Conference, OTC-18063 (2006)

[14] Chen A. and Chia H.K., Pipe-in-Pipe Walking: Understanding the Mechanism, Evaluating and Mitigating the Phenomenon

[15] Goplen S., Fyrileiv O., Grandal J.P. and Borsheim L., Global Buckling of Pipe-in-Pipe – Structural Response and Design Criteria, Proceedings of the 30th International Conference on Ocean, Offshore and Arctic Engineering, OMAE2011-49960 (2011)

[16] Fyrileiv O., Marley M. and Pettersen S., Design Methodology for Axial Force Response of Pipe-in-Pipe – A Probablistic Approach, Proceedings of the 30th International Conference on Ocean, Offshore and Arctic Engineering, OMAE2011-49184 (2011)

[17] Bokaian A., Thermal Expansion of Pipe-in-Pipe Systems, Marine Structures vol. 17, pp. 475-500 (2004)

[18] Sriskandarajah T., Ragupathy P., Anurudran G., Challenges in the Design of HP/HT Pipelines, Proceedings of the 23rd Annual Offshore Pipeline Technology Conference, OPT, pp. 1-33 (2000)

[19] Duffy B.W., Lee L.H. and Brunner M., Thermal Expansion and Helical Buckling of Pipe-in-Pipe Flowline Systems, Proceedings of the 2012 Simulia Customer Conference (2012)

[20] Dixon M., Jackson D. and El-Chayeb A., Deepwater Installation Techniques for Pipe-in-Pipe Systems Incorporating Plastic Strains, Proceedings of the Offshore Technology Conference, OTC-15373 (2003)

[21] Giagmouris T., Qi X., Tang A ; and Zhong J., Response and Simulation of the Pipe-in-Pipe Systems in Free Spans, Proceedings of the Offshore Technology Conference, OTC-24073 (2013)

[22] Giagmouris T., Qi X., Tang A; and Zhong J., Mechanical Behaviour of a Pipe-in-Pipe System in a Span, Proceedings of the 2013 Simulia Community Conference (2013)

[23] Van den Abeele F. and Denis R., Recent Developments in Numerical Modelling and Analysis for Offshore Pipeline Design, Installatoin and Operation, Journal of Pipeline Engineering, JPE Q4, pp. 273-286 (2012)

[24] Van den Abeele F., Boël F. and Hill M., Fatigue Analysis of Free Spanning Pipees subjected to Vortex Induced Vibrations, Proceedings of the 32nd International Conference on Ocean, Offshore and Arctic Engineering, OMAE2013-106325 (2013)

[25] Det Norske Veritas, Recommended Practice DNV-RP-F105, Free Spanning Pipelines (2006)

[26] Kurusami D., Thin Wall Approximation: Implications for the Expansion and Global Buckling of Thick Walled, High Pressure Flowlines, Proceedings of the Offshore Technology Conference, OTC-24028 (2013)